Hindawi Publishing Corporation
Advances in Condensed Matter Physics
Volume 2015, Article ID 320187, 5 pages
http://dx.doi.org/10.1155/2015/320187

Research Article

Low-Temperature DC Carrier Transport in $(Fe_{0.45}Co_{0.45}Zr_{0.10})_x(Al_2O_3)_{1-x}$ Nanocomposites Manufactured by Sputtering in Pure Ar Gas Atmosphere

Ivan A. Svito,[1] Alexander K. Fedotov,[1] Anis Saad,[2] Momir Milosavljević,[3] Julia A. Fedotova,[4] Tomasz N. Kołtunowicz,[5] and Paweł Żukowski[5]

[1]*Belarusian State University, Independence Avenue 4, 220030 Minsk, Belarus*
[2]*Physics Department, Al Balqa Applied University, P.O. Box 4545, Amman 11953, Jordan*
[3]*Vinča Institute of Nuclear Sciences, Belgrade University, 11001 Belgrade, Serbia*
[4]*National Centre for Particles and High Energy Physics of Belarusian State University, Bogdanovich 153, 220040 Minsk, Belarus*
[5]*Lublin University of Technology, 38a Nadbystrzycka Street, 20-618 Lublin, Poland*

Correspondence should be addressed to Tomasz N. Kołtunowicz; t.koltunowicz@pollub.pl

Received 24 November 2014; Accepted 4 February 2015

Academic Editor: Ram N. P. Choudhary

This presented work investigates the structure and temperature relationship/dependence of the DC conductivity $\sigma(T)$ in the $(Fe_{0.45}Co_{0.45}Zr_{0.10})_x(Al_2O_3)_{1-x}$ nanocomposites deposited in Ar atmosphere with composition ($30 < x < 100$ at.%) and temperature ($2 < T < 300$ K). It is shown that VRH $\sigma(T)$ displayed crossover from Mott-like to Shklovskii-Efros regimes which occurred at temperatures of 100–120 K. It is also noted that the observed shift of the percolation threshold to higher concentrations of metallic fraction can be attributed to the disordering of the metallic nanoparticles due to the incorporation of the residual oxygen in the vacuum chamber during the deposition procedure.

1. Introduction

Composite materials consisting of ferromagnetic nanoparticles embedded into a dielectric matrix have occupied one of the center places in physics research at present time because of the challenges regarding the theoretical understanding and practical applications [1]. There are two reasons for this interest: the tendency to miniaturization of the electromagnetic devices and improvement of their performance [2] and the lack of understanding regarding the low-temperature carrier transport mechanisms in many of metal-dielectric composites, when dimensions of the metallic phase particles are approaching the nanometer scale. The characteristics of the DC carrier transport in nanocomposites containing metallic nanoparticles randomly distributed in dielectric matrix should be strongly dependent on the composition of the material and, in particular, on the position of percolation threshold x_C. The latter is determined by atomic fraction of the metallic phase x in the composite, ratio of conductivities of metallic and dielectric phases, phase composition of nanoparticles (the presence or lack of native oxides around them), matrix, and also some geometrical parameters of metallic phases (dimensions and their scattering, shape and topology of distribution of nanoparticles, etc.) [2–5].

The present paper is devoted to the study of the temperature and magnetic field dependence of DC resistivity in $(Fe_{0.45}Co_{0.45}Zr_{0.10})_x(Al_2O_3)_{1-x}$ nanocomposites, deposited in Ar atmosphere, depending on their position relative to the percolation threshold.

2. Materials and Methods

The $(Fe_{0.45}Co_{0.45}Zr_{0.10})_x(Al_2O_3)_{1-x}$ nanocomposites thin films with $0.28 < x < 1.00$ and thicknesses d of 1–4 μm were fabricated by DC ion sputtering of the compound target onto the motionless glass ceramic substrate (25 cm × 5 cm), using 2 keV argon ion gun, at the rate of 0.28 nm·s^{-1}. Sputtered

targets were composed of $Fe_{0.45}C_{0.45}Zr_{0.10}$ alloy plates, covered with strips of amorphous Al_2O_3 that were pasted on top. The deposition was made in a vacuum chamber evacuated down to 1×10^{-4} Pa and then filled with pure argon up to a total gas pressure of $(6.7–9.6) \times 10^{-2}$ Pa. In this way, by changing the area coverage of the constituents, the metal/insulator compositional ratio in the deposited films could be varied [6].

The as-deposited granular films were subjected to the study of the structure and composition (see [3]), using the LEO 1455VP scanning electron microscope (SEM) with a special energy dispersive X-ray (EDX) microprobe, X-ray Empyrean PAN analytical diffractometer (XRD), Mössbauer spectrometer MS2000 with ^{57}Fe/Rh source, and Rutherford backscattering spectrometry (RBS), and microstructural studies with electron diffraction (SAED) were also done using Philips EM400T transmission electron microscope (TEM), operated at 120 kV, and Philips CM200 operated at 200 kV for high resolution analysis (HRTEM). EDX SEM and RBS measurements were performed for checking the samples' stoichiometry with accuracy of ~1%, confirming x and Fe/Co/Zr relation close to the nominal [6]. Thicknesses of the films were measured using SEM with accuracy of ~2-3% on cleavages of the samples studied.

For electric measurements the nanocomposite films were cut into rectangular strips with dimensions of 10 mm × 2 mm × d μm, and 4 indium contacts were deposited using ultrasound soldering. These samples were used for four-probe DC conductivity σ measurements at low electric field intensities of $E < 10^5$ V/m when I-V characteristics were practically linear. Magnetoresistivity measurements were performed with the current perpendicular to the applied magnetic fields. Dependence of σ on temperature (between 2 and 300 K) was measured using a closed-cycle cryogen-free cryostat system (Cryogenic Ltd., London). The PC based control system with Lakeshore Temperature Controller (Model 331) allowed to scan the temperature with a rate of 0.1–1 K/min and to stabilize it (if necessary) with accuracy of 0.005 K. The relative error of conductance measurements was less than 0.1%.

3. Results and Discussion

The comparison of SEM, XRD, TEM, SAED, and Mössbauer data for the studied samples, presented in [6], drew the following conclusions concerning their phase structure. Mössbauer and also magnetization studies are evident of strong correlation between the magnetic state and concentration of the metallic fraction in the composites: the samples with $x < 0.43–0.45$ were in the superparamagnetic state whereas the samples with higher x values showed the ferromagnetic behavior [5, 6]. Therefore, concentration of the order of 0.43–0.45 can be interpreted as the percolation threshold x_C when $Fe_{0.45}Co_{0.45}Zr_{0.10}$ nanoparticles begin to form percolating (highly conductive) net in alumina matrix. TEM and HRTEM images revealed that the granular films with $x < x_C$ contain crystalline metallic *bcc* α-FeCo-based nanosized cores embedded in the amorphous Al_2O_3 matrix (see Figure 1). A bcc structure of these nanoparticles

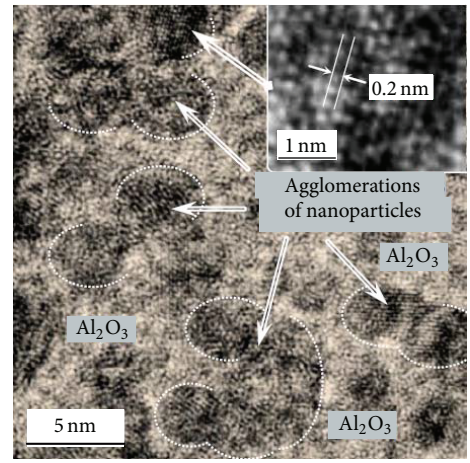

Figure 1: HRTEM and TEM images for the film of $x = 0.42$.

(close to a pure reference $Fe_{0.45}Co_{0.45}Zr_{0.10}$ alloy film) and their random orientation were also revealed by XRD and SAED measurements [5, 6]. Figure 1 shows that the alloy nanoparticles have tendency for agglomeration. Moreover, XRD has shown that the metallic nanoparticles are highly disordered (probably due to the incorporation of the residual oxygen atoms presented in the vacuum chamber) displaying increased lattice parameters as compared to that for pure FeCoZr films deposited at the same regimes.

The measured dependence of conductivity σ on concentration x of metallic fraction ($Fe_{0.45}Co_{0.45}Zr_{0.10}$ alloy) in the studied films is shown in Figure 2. The figure indicates that both of $\sigma(x)$ curves, measured at 2.2 K and 300 K, display monotonous (close to sigmoid-like) behavior with inflection point that is characteristic for percolating systems [7]. However, the characteristics of $\sigma(x)$ curves measured at low and high temperatures have some peculiarities. One of them is that, for the 300 K (see Figure 2(a)), the difference in conductivities for the low-x (~0.31–0.32) and high-x (>0.55) is approximately 3 orders of magnitude, whereas, for the 2.2 K (see Figure 2(b)), it exceeds 12 orders of magnitude. In the clearest form this is also seen by comparing the inserts of Figures 2(a) and 2(b), where 2nd derivatives $\sigma'' = d^2\sigma/dx^2$ are presented (derived by graphical differentiation). The inserts show the $\sigma''(x)$ curves exhibiting maxima at the concentrations x_{max} of 0.48 to 0.51. Positions of x_{max} lie a little higher than the percolation threshold $x_C \approx 0.43–0.45$, determined by Mössbauer and magnetization experiments [6]. Comparison of the $\sigma''(x)$ dependence for the two temperatures allows separating the $\sigma(x)$ behavior/progress with the metallic fraction concentration in the nanocomposites into 3 characteristic parts. It can be seen that region A has a smooth increase of σ with x up to the kinks at $x \sim 0.45$ of $\sigma''(x)$ curve in Figures 2(a) and 2(b). After the kinks, in the intermediate region B with $0.4 < x < x_{max}$, every $\sigma''(x)$ curve in the inserts has higher slope than that in region A. When x reaches x_{max} $\sigma''(x)$ curves fall down (see part C in the inserts in Figures 2(a) and 2(b)).

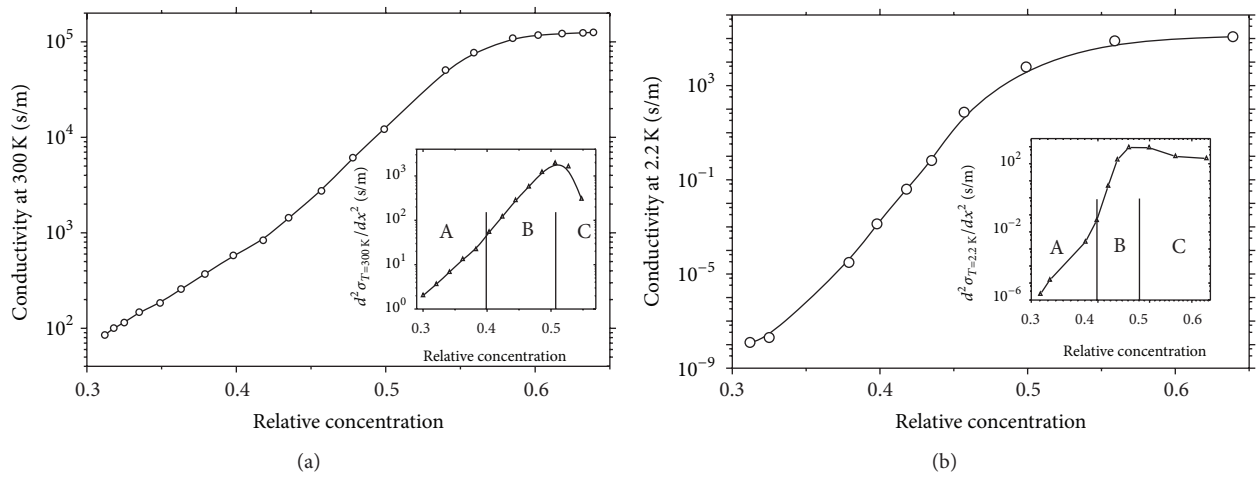

FIGURE 2: Dependence of DC conductivity and their second derivatives $\sigma'' = d\sigma^2/dx^2$ measured at temperatures of 298 K (a) and 2.2 K (b) on the metal-to-dielectric ratio x for the as-deposited films. $\sigma''(x)$ dependence is presented in the inserts.

Temperature dependence of the DC conductivity is presented in Figure 3 in Arrhenius and normalized scales. Analysis of the $\sigma(T)$ curves shows that they are strongly different for the 3 regions of x values mentioned above. Figure 3(a) shows that the samples of regions A and B, indicated in Figure 2, display $\sigma(T)$ dependence with $(d\sigma/dT) > 0$ and that is the characteristic of the thermally activated carrier transport on the insulating side of the insulator-metal transition (IMT). In doing so, the samples of region A were characterized with higher slopes in the low-temperature range (see curves 1–3 in Figure 3(a)) whereas positive values of $(d\sigma/dT)$ for the samples of region B have lower slopes (curves 4–6). Curve 7 in Figure 3(a), for the sample approaching region C in Figure 2 with $x > x_{max}$, also displays positive values of $(d\sigma/dT)$ (but close to zero). Moreover, curve 8 in the region C, presented in the normalized form in Figure 3(b), shows $(d\sigma/dT) \leq 0$. This allows concluding that beyond the x_{max} transition to metallic temperature dependence of the conductivity though power-like $\sigma(T)$ dependence (as in the films of pure FeCoZr alloy deposited in the same sputtering conditions, see curve 9 in Figure 3(b)) was not observed.

The obtained $\sigma(x, T)$ curves for the studied samples, belonging to different regions A, B, and C in the inserts in Figures 2(a) and 2(b), can be discussed according to the carrier transport mechanisms theory. The experimental curves 1–6 in Figure 3(a), plotted in Arrhenius scale, show that the samples with $x < x_{max} \approx 0.48$–0.51 exhibited exponential-like character of $\sigma(T)$ dependence where the activation energy changed (reduced) as the temperature decreased. Such behavior means that the samples of regions A and B lie on the dielectric side of the IMT indicating hopping mechanism of conductance. The conductance $\sigma(T)$ dependence for the samples of region C (curve 7 in Figure 3(a) and curve 8 in Figure 3(b)) exhibited practically zero values of $d\sigma/dT$ denoting transition of the nanocomposites to the state close to the metallic one.

To understand the nature of activation law of $\sigma(T)$ dependence for the samples of regions A and B (insulating side of IMT) in Figure 3, curves were replotted as $\sigma(T)$ in Mott scales in accordance with the known relation

$$\rho(T) = \rho_0 \exp\left(-\left(\frac{T_0}{T}\right)^n\right) \quad (1)$$

for variable range hopping (VRH) conductance (see Figure 4). The ρ_0 and T_0 are characteristic parameters of the hopping models. The exponent n in (1) depends on VRH regime: $n = 0.25$ is used for Mott mechanism [8] and $n = 0.50$ corresponds to Shklovskii-Efros model [9]. Results of the presented experiments for the studied composites have shown that Mott law was observed at temperatures higher than 110–120 K and changed to the Shklovskii-Efros law, describing the hopping transport of the charge carriers at the Coulomb gap in the dense localized states, as temperature decreased.

The above-mentioned results indicated that the concentration x_{max}, where $\sigma''(x)$ curves exhibited maxima, can be considered as the percolation threshold. Therefore, behavior of $\sigma(T)$ in region C (curves 7 and 8 in Figure 3) can be attributed to the carrier transport along the percolating net of FeCoZr nanoparticles which is fully completed in this region of x. On the other side, shift of x_{max} to higher concentrations should be noted as compared with x_C values (0.43–0.45) observed in [5, 6]. The value of x_{max} is close to 0.5 that corresponds to 3D model of percolation for the binary composites metal-insulator [10]. This shift and the practical zero values of $d\sigma/dT$ can be attributed to the partially disordered state of the metallic nanoparticles (at least, at the interface nanoparticle/matrix) probably due to their enrichment by the residual oxygen in vacuum chamber.

4. Conclusions

It was shown that the temperature dependence of the DC conductivity $\sigma(T)$ in the $(Co_{0.45}Fe_{0.45}Zr_{0.10})_x(Al_2O_3)_{1-x}$ nanocomposites, deposited in Ar atmosphere and being on

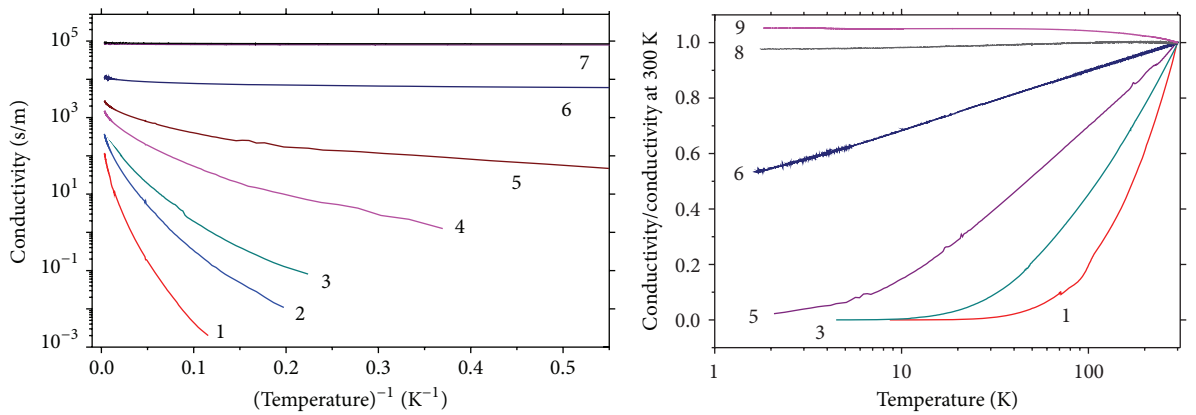

FIGURE 3: Dependence of DC conductivity $\sigma(T)$ *versus* temperature in Arrhenius scale (a) and in the normalized form $\sigma(T)/\sigma(300\,\mathrm{K})$ (b) for $x = 0.325$ (1), 0.380 (2), 0.398 (3), 0.440 (4), 0.457 (5), 0.496 (6), 0.560 (7), 0.640 (8), and 1.000 (9).

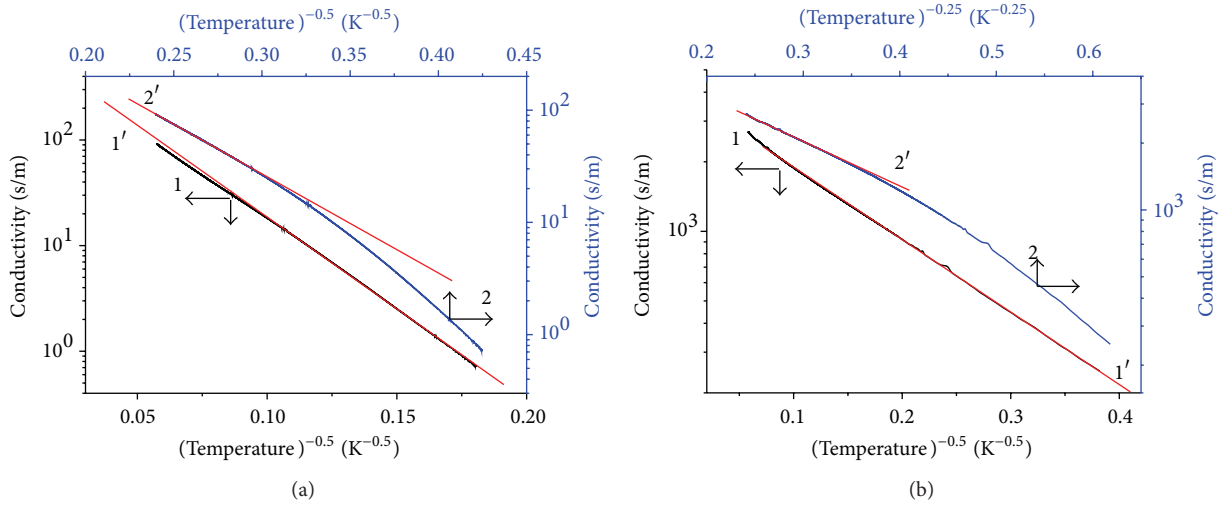

FIGURE 4: Temperature dependence of conductivity $\sigma(T)$ for the samples of $x = 0.312$ (a) and 0.457 (b) plotted in Mott scale with the exponent $n = 0.5$ (curves 1 and 1′) and $n = 0.25$ (curves 2 and 2′) in relation (1). 1, 2—experimental data and 1′, 2′—linear approximations of $\ln \rho - T^{-n}$ with $n = 0.5$ and $n = 0.25$ correspondingly.

dielectric side of IMT, displayed crossover from Mott-like to Shklovskii-Efros VRH regimes which occurred at temperatures about 100–120 K.

Shift of the percolation threshold, as observed from the $\sigma(x, T)$ dependence, to the higher metallic fractional concentrations compared to that in [5, 6] can be attributed to the disordering of the metallic alloy nanoparticles due to the incorporation of the residual oxygen in the vacuum chamber during the deposition procedure.

Conflict of Interests

The authors declare that there is no conflict of interests regarding the publication of this paper.

Acknowledgments

The work was partially supported by the VISBY Program of the Swedish Institute and Belarusian State Sub-Programme "*Crystalline and Molecular Structures*" by Contract 2.4.12.

References

[1] Y. Imry, in *Nanostructures and Mesoscopic Systems*, W. P. Kirk and M. A. Reed, Eds., p. 11, Academic Press, New York, NY, USA, 1992.

[2] G. Timp, *Nanotechnology*, Springer, New York, NY, USA, 1999.

[3] T. N. Koltunowicz, P. Zukowski, M. Milosavljević et al., "AC/DC conductance in granular nanocomposite films $(Fe_{45}Co_{45}Zr_{10})_x(CaF_2)_{100-x}$," *Journal of Alloys and Compounds*, vol. 586, supplement 1, pp. S353–S356, 2014.

[4] T. N. Kołtunowicz, P. Zhukowski, V. V. Fedotova, A. M. Saad, A. V. Larkin, and A. K. Fedotov, "The features of real part of admittance in the nanocomposites $(Fe_{45}Co_{45}Zr_{10})_x(Al_2O_3)_{100-x}$ manufactured by the ion-beam sputtering technique with Ar ions," *Acta Physica Polonica A*, vol. 120, no. 1, pp. 35–38, 2011.

[5] J. A. Fedotova, "FeCoZr-Al_2O_3 granular nanocomposite films with tailored structural, electric, magnetotransport and magnetic properties," in *Advances in Nanoscale Magnetism*, vol. 122 of *Springer Proceedings in Physics*, pp. 231–267, Springer, Berlin, Germany, 2009.

[6] J. A. Fedotova, J. Przewoznik, C. Kapusta et al., "Magnetoresistance in $FeCoZrAl_2O_3$ nanocomposite films containing metal coreoxide shell nanogranules," *Journal of Physics D: Applied Physics*, vol. 44, no. 49, Article ID 495001, 2011.

[7] A. L. Efros and B. I. Shklovskii, "Critical behaviour of conductivity and dielectric constant near the metal-non-metal transition threshold," *Physica Status Solidi (B) Basic Research*, vol. 76, no. 2, pp. 475–485, 1976.

[8] N. F. Mott and E. A. Davis, *Electron process in non-crystal line materials*, Claredon Press, Oxford, UK, 1979.

[9] A. L. Efros and B. I. Shklovskii, "Coulomb gap and low temperature conductivity of disordered systems," *Journal of Physics C: Solid State Physics*, vol. 8, no. 4, pp. L49–L51, 1975.

[10] G. Grimmett, *Percolation*, Springer, Berlin, Germany, 1999.